Apoptosis (2008) 13:993–1004
DOI 10.1007/s10495-008-0231-8

ORIGINAL PAPER

Molecular mechanism underlying differential apoptosis between human melanoma cell lines UACC903 and UACC903(+6) revealed by mitochondria-focused cDNA microarrays

Qiuyang Zhang · Jun Wu · AnhThu Nguyen · Bi-Dar Wang · Ping He · Georges St. Laurent · Owen M. Rennert · Yan A. Su

Published online: 19 June 2008

Abstract Human malignant melanoma cell line UACC903 is resistant to apoptosis while chromosome 6-mediated suppressed cell line UACC903(+6) is sensitive. Here, we describe identification of differential molecular pathways underlying this difference. Using our recently developed mitochondria-focused cDNA microarrays, we identified 154 differentially expressed genes including proapoptotic (BAK1 [6p21.3], BCAP31, BNIP1, CASP3, CASP6, FAS, FDX1, FDXR, TNFSF10 and VDAC1) and antiapoptotic (BCL2L1, CLN3 and MCL1) genes. Expression of these pro- and anti-apoptotic genes was higher in UACC903(+6) than in UACC903 before UV treatment and was altered after UV treatment. qRT-PCR and Western blots validated microarray results. Our bioinformatic analysis mapped these genes to differential molecular pathways that predict resistance and sensitivity of UACC903 and UACC903(+6) to apoptosis respectively. The pathways were functionally confirmed by the FAS ligand-induced cell death and by siRNA knockdown of BAK1 protein. These results demonstrated the differential molecular pathways underlying survival and apoptosis of UACC903 and UACC903(+6) cell lines.

Keywords Melanoma · Apoptosis · Pathways · FAS · FASLG · BAK1

Qiuyang Zhang, Jun Wu, and AnhThu Nguyen made equal contributions to this work.

Electronic supplementary material The online version of this article (doi:10.1007/s10495-008-0231-8) contains supplementary material, which is available to authorized users.

Q. Zhang · J. Wu · A. Nguyen · B.-D. Wang · G. St. Laurent · Y. A. Su (✉)
Department of Biochemistry and Molecular Biology and the Catherine Birch McCormick Genomics Center, The George Washington University School of Medicine and Health Sciences, Ross Hall, Room 555, 2300 I Street NW, Washington, DC 20037, USA
e-mail: bcmyas@gwumc.edu

P. He
Laboratory of Cellular Hemostasis, Division of Hematology, Center for Biological Evaluation and Research, Food and Drug Administration, Bethesda, MD 20892, USA

G. St. Laurent
Immunovirology - Biogenesis Group, University of Antioquia, A.A. 126, Medellin, Colombia

O. M. Rennert
Laboratory of Clinical Genomics, Eunice Kennedy Shriver National Institute of Child Health and Human Development, National Institutes of Health, Bethesda, MD 20892, USA

Introduction

Human cutaneous malignant melanoma (CMM) reigns as the most deadly form of skin cancer, responsible for 75% of all skin cancer-related deaths [1]. The incidence of melanoma continues to increase in western populations—the number of cases worldwide has doubled in the past 20 years [2]. CMM frequently results from transformation of melanocytes in the skin. High resistance to treatment is a unique hallmark of malignant melanoma, although the mechanisms by which melanoma cells protect themselves against induced apoptosis remains largely unknown [3]. Many tumor cells bypass the apoptotic machinery through mechanisms that may involve dysregulation of pro- and anti-apoptotic genes [4]. Cytogenetic and molecular studies have mapped frequent chromosomal breaks and deletions on chromosomes 1, 6, 7, 9, 10, 11, and 19, and associated these abnormalities with the development and progression

of CMM [5–7]. In particular, chromosome 6 abnormalities have been found in >80% cases [8–11] and are believed to play a key role in progression of CMM. Supporting this notion, introduction of a *neo*-tagged normal chromosome 6 into human malignant melanoma cell lines results in suppression of tumorigenicity [12] and metastasis [13, 14], and enhancement of apoptosis [15]. These structural and functional studies strongly suggest that multiple genes on chromosome 6 play a causal role in the development and progression of CMM.

The genetically linked human melanoma cell lines UACC903 and UACC903(+6) phenotypically exhibit distinctive characteristics. Specifically, the parental UACC903 cell line demonstrates rapid population-doubling time, focus formation in monolayer culture, anchorage-independent growth, and rapid formation of s.c. tumors in athymic nude mice. In contrast, the UACC903(+6) cell subline shows suppression of all these phenotypes [12]. Using these two cell lines, we previously identified the chromosome 6-encoded tumor suppressor gene connexin 43 which partially explains the suppression of tumorigenic phenotypes as a consequence of the introduced chromosome 6 [16, 17]. Recently, we demonstrated significant differences between UACC903 and UACC903(+6) cell lines in apoptosis and cell distribution in G0/G1-, S- and G2/M-phases of the cell cycle before and after UV irradiation [15]. The apparent apoptotic difference strongly suggests the presence of differential molecules that regulate survival and apoptosis.

In this report, we describe the identification of differentially expressed genes in the survival-apoptosis signaling pathways that account for differences in apoptosis between UACC903(+6) and UACC903 cell lines before and after UV irradiation. Using human mitochondria-focused cDNA microarrays [18], we identify gene expression profiles before (0-h) and at 1.5-, 3-, 6- and 12-h after UV treatment. After qRT-PCR validation of microarray results, we identified 154 differentially expressed genes of which 104 changes their expression in response to UV treatment, suggesting differential regulation in these two cell lines. Bioinformatics analysis revealed 16 genes relevant to proapoptosis, 3 to antiapoptosis, 5 to DNA damage repair and 1 to the G2 check point. We mapped these proapoptotic and antiapoptotic genes to known survival-apoptosis signaling pathways. Western blots confirmed expression changes of proapoptotic proteins BAK1 (encoded by chromosome 6p21.3) and FAS, and antiapoptotic proteins BCL2L1 and MCL1. Our MTS assay revealed that the FAS ligand (FASLG)-induced cell death was both dose- and time- responsive in these two cell lines. Moreover, siRNA knockdown of the BAK1 protein in UACC903(+6) cells resulted in increased survival and attenuation of FASLG-induced cell death. These results demonstrate chromosome 6-encoded BAK1-involved differential survival-apoptosis signaling pathways as the molecular mechanism underlying resistance and sensitivity to apoptosis of human CMM cell line UACC903 and the chromosome 6-mediated suppressed cell subline UACC903(+6). These pathways have implications for therapeutic research.

Methods and materials

Cell culture

UACC903 and UACC903(+6) cell lines were originally obtained from University of Arizona Cancer Center [12]. UACC903 cells were cultured in RPMI1640 with 10% fetal bovine serum, 2 mM L-glutamine. UACC903(+6) cells were cultured in the same medium with 600 μg/ml G418 to select for the pSV2*neo*-tagged chromosome 6.

UV irradiation

After removing medium, cells at 90% confluence in 100-mm dishes were exposed to UV (254 nm) generated by UV Crosslinker (Model BLX254, Life Technologies, Gaithersburg, MD) at the dose of 40-J/M^2. Medium was added immediately to continue culture until designated time points. Cells at 0 h had no UV treatment.

Flow cytometry

It was performed by previously described methods [19, 20]. Both attached and floating cells were harvested for cell cycle analysis. For each experiment, 10,000 cells were analyzed using ELITE Flow Cytometry (Beckman Coulter, Fullerton, CA) and Cell Quest software (Becton Dickinson, Franklin Lakes, NJ).

TUNEL assay

Terminal DNA transferase-mediated dUTP biotin nick end labeling (TUNEL) assay was employed to determine in situ apoptotic DNA breaks [21, 22] by using the Detection Kit (Roche Applied Sciences, Germany) following manufacturer's instructions. Cells attached to glass slides in culture dishes were subjected to TUNEL assay and were then analyzed under Olympus BX 60 fluorescent microscope using Evolution CCD System and ImagePro software (Media Cybernetics, Rockville, MD).

hMitChip3 microarray

A third-generation human mitochondria-focused cDNA microarray (hMitChip3) containing 37 mitochondrial DNA-encoded genes, 1,098 nuclear DNA-encoded and

mitochondria-related genes and 225 controls were printed as described previously [18]. Total RNA was extracted using Trizol reagent (Invitrogen) and purified with RNeasy kit (Qiagen, Valencia, CA), as previous description [23]. Ten micrograms of RNA per sample were used for microarray labeling and hybridization as previously described [18]. Slides were scanned using the ScanArray Express Microarray Scanner (PerkinElmer, Boston, MA) as described previously [18].

Microarray data analysis

Microarray database construction, data filtering and normalization were performed as described previously [18]. The normalized data were used to cluster genes by using Eisen's Cluster software [24] and to calculate differentially expressed genes. Heat map was visualized by using Maple Tree (http://rana.lbl.gov/EisenSoftware.htm). Gene identifiers including clone ID, accession number, Unigene ID, gene ID, symbol and name were updated according to human UniGene Build 204 (ftp://ncbi.nih.gov/repository/UniGene/). Gene ontology and pathways were downloaded from Entrez (ftp://ncbi.nlm.nih.gov/gene). Ingenuity Pathway Analysis software IPA 5.0 (Redwood City, CA) was used to map pathways.

Quantitative RT-PCR (qRT-PCR)

Two micrograms of total RNA per sample were reverse-transcribed into cDNA by using SuperScript^{TM} First-Strand Synthesis System (Invitrogen). Thirty nanograms of each cDNA sample was used for 40 cycles of qPCR analysis with the Universal PCR Master Mix on an Applied Biosystems 7300 Real Time PCR System and Software (Applied Biosystems, Foster City, CA), following the manufacturer instructions. Triplicate qPCR experiments were performed for each gene. Relative RNA concentrations were calculated using the published methods [23, 25]. TaqMan probes and primers for glyceraldehyde-3-phosphate dehydrogenase (GAPDH, 4352934E); Fanconi anemia complementation group D2 (FANCD2, Hs00276992_m1); DEAH (Asp-Glu-Ala-His) box polypeptide 16 (DHX16, Hs00374356_m1); adenosylmethionine decarboxylase 1 (AMD1, Hs00750876_s1); BCL2-like 1 (BCL2L1, Hs99999146_m1); uracil-DNA glycosylase (UNG, Hs00422172_m1); Fas TNF receptor superfamily member 6 (FAS, Hs00531110_m1); BCL2-antagonist/killer 1 (BAK1, Hs00832876_g1); caspase 3 apoptosis-related cysteine peptidase (CASP3, Hs00234387_m1); protein phosphatase 2 catalytic subunit alpha isoform (PPP2CA, Hs00427259_m1); and myeloid cell leukemia sequence 1 (MCL1, Hs03043898_m1) were purchased from Applied Biosystems.

FAS ligand (FASLG)-induced apoptosis

Human recombinant soluble FASLG was purchased from the Kamiya Biomedical Company (Seattle, WA). 4,000 and 5,000 cells in 20-μl media were plated into a 96 well plate for cell lines UACC903 and UACC903(+6), respectively. The dose-response curves were determined for FASLG at the final concentrations of 0, 50, 100, 200 and 400 ng/ml. Cells were incubated for 22 h after addition of FASLG and viable cells were measured by MTS cell proliferation assay. The time–response curves were determined for 100 ng/ml of FASLG at the time points of 0, 1.5, 3, 6, 12, and 24 h after UV treatment.

MTS cell proliferation assay

The CellTiter 96 AQueous One Solution Cell Proliferation Assay kit (Promega, Madison, WI) was used to assess number of viable cells following manufacturer's instructions. Twenty microliters MTS reagent was added to cells in 100-μl media in a well of 96-well plates. After incubation at 37°C (5% CO_2) for 2 h, viable cells were measured at 490-nm absorbance with spectrophotometer SPECTRAmax (Molecular Devices, Sunnyvale, California). Background absorbance was recorded with control cells. After subtraction of the background, absorbance was converted to cell number based on standard curves generated from UACC903 and UACC903(+6) cells for plotting dose– and time–response curves.

siRNA experiments

BAK1 siRNA duplex, transfection reagents and mock control (non-specific siRNA) were purchased from Ambion (Austin, TX) and used following the manufacturer's instructions. Briefly, transfection and knockdown efficiencies of siRNA were optimized as 6×10^5 cells/ml for UACC903(+6) by use of the manufacturer-provided GAPDH siRNA and KDalert GAPDH Assay Kit. At 80–90% confluence, cells in monolayer culture were lifted with 0.05% Trypsin. Cell numbers were determined by use of a Coulter Particle Counter (Model Z18, Beckman-Coulter Inc., Miami, FL). Transfection reagents (siPORT NeoFX) and stock siRNA were combined and incubated at room temperature for 45-min. Twenty microliters of siPORT NeoFX and siRNA (40 nM final concentration) reaction mixture was placed into each well of a 96 well plate, followed by addition of 80-μl cell suspension. After incubation for 48 h, 20-μl MTS reagent was added to measure viable cells at 490-nm absorbance with spectrophotometer SPECTRAmax (Molecular Devices). All experiments were performed in triplicate.

Western blots analysis

Cells were harvested at indicated time points. Protein concentration of cell lysate was determined by using DC Protein Assay Kit (Bio-Rad, Hercules, CA). Approximately 30 μg of protein were subjected to electrophoresis in 12% denatured SDS-polyacrylamide gel. Proteins in gel were transferred to the Improved Polyscreen PVDF Transfer Membrane (PerkinElmer Life Science Inc., Boston, MA) as described by the manufacturer. Mouse monoclonal antibodies (anti-FAS [B-10, Cat.# sc-8009] and anti-BCL2L1 [H-5, Cat.# sc-8392]) and rabbit polyclonal antibodies (anti-BAK1 [H-211, Cat.# sc-7873] and anti-MCL1 [k-20, Cat.# sc-958]) were from Santa Cruz Biotechnology (Santa Cruz, CA); and mouse monoclonal antibody (anti-GAPDH [6c5, Cat.# AM4300]) was from Ambion (Austin, TX). BAK1, FAS, MCL1 and BCL2L1 antibodies were diluted at 1:500 and GAPDH antibody was diluted at 1:20,000 to detect the corresponding proteins. Secondary antibodies used were horseradish peroxidase-conjugated anti-rabbit or anti-mouse antibodies (Santa Cruz Biotechnology). Blots were visualized by the ECL Western blotting detection reagents (PerkinElmer LAS, Austin, TX) and X-ray films. Images were scanned and quantified by using Scanalytics IPLAB 3.6 (Rockville, MD).

Statistics

Statistical calculations were performed on triplicate array experiments using XLSTAT 2006 (XLSTAT, New York, NY). Differentially expressed genes were identified by equal to or greater than 1.5-fold change in the average expression of the background-subtracted mean intensity ratios of a gene between cell lines and/or between time points. The level of statistical significance was set at a P-value <0.05.

Results

Apoptosis of UACC903(+6) and G2/M arrest of UACC903 before and after UV treatment

To characterize apoptotic responses of human malignant melanoma cell line UACC903 and chromosome 6-mediated suppressed cell subline UACC903(+6), we compared apoptosis rates and distribution rates of cells in the cell cycle derived from TUNEL assay and flow cytometry, respectively. The results indicated that TUNEL-positive apoptotic cells were $2.3 \pm 0.6\%$ in the UACC903 population and $9.6 \pm 1.1\%$ in the UACC903(+6) before UV irradiation ($P < 0.001$), compared to $12.1 \pm 2.1\%$ and $51.0 \pm 8.9\%$, respectively, 12 h after UV treatment ($P < 0.0001$) (Fig. 1). The levels of G2/M arrested cells exhibited another major difference between the two cell lines. The G2/M-phase cells were $16.9 \pm 0.3\%$ in the UACC903 population and $13.2 \pm 0.5\%$ in UACC903(+6) before UV treatment ($P < 0.001$), compared to $27.0 \pm 0.7\%$ and $15.7 \pm 0.1\%$, respectively, 24 h after UV treatment ($P < 0.001$). Thus, while apoptosis occurred in UACC903(+6) cells, G2/M arrest was a major event in UACC903 cells.

Expression clusters of 154 genes in UAC903(+6) and UACC903 cells before and after UV treatment

To investigate the molecular mechanism underlying the differential apoptosis between UACC903 and UACC903 (+6), we identified expression profiles of 154 significantly ($P < 0.05$) differentially expressed genes between these two cell lines before and at 1.5, 3, 6 and 12 h after UV treatment using the hMitChip3 microarray (Supplemental Table 1). Our unsupervised clustering analysis of these 154 genes revealed 3 (A, B, and C) clusters and 9 (A-1 through A-4, B-1 through B-3 and C-1 to C-2) sub-clusters (Fig. 2). Without UV treatment, the expression levels of genes in A, B and C clusters in UACC903(+6) were higher than, equal

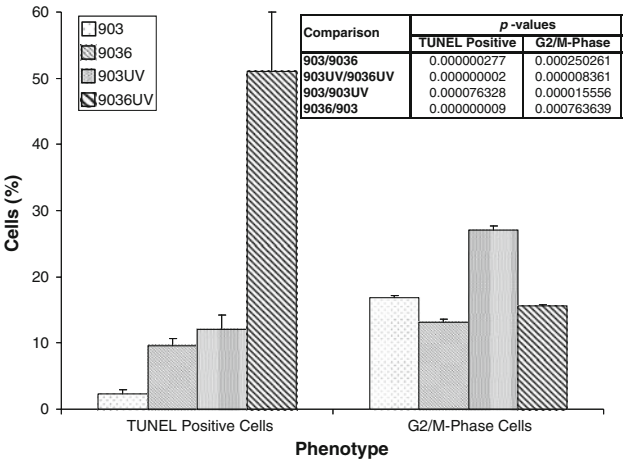

Comparison	p-values	
	TUNEL Positive	G2/M-Phase
903/9036	0.000000277	0.000250261
903UV/9036UV	0.000000002	0.000008361
903/903UV	0.000076328	0.000015556
9036/903	0.000000009	0.000763639

Fig. 1 Bar graph of the TUNEL-positive apoptotic cells and G2/M phase cells before and after UV irradiation. TUNEL-positive cells: UACC903 and UACC903(+6) cells before and at 12 h after the UV irradiation were processed by the terminal deoxynucleotidyl transferase-mediated dUTP biotin nick-end labeling (TUNEL) assay using the In Situ Cell Death Detection Kit (TMR, Roche). On average, 700 cells were analyzed for each of triplicate experiments to calculate means and SD of the TUNEL-positive cells. G2/M-phase cells: UACC903 and UACC903(+6) cells were sorted based on DNA contents after staining, with propidium iodide (PI), UACC903 and UACC903(+6) cells before and at 12 h after the UV irradiation. 10,000 cells were sorted using ELITE Flow Cytometry (Beckman Coulter) and analyzed with Cell Quest software (Becton Dickinson). Means and SD were calculated from triplicate experiments. The P-values between comparisons are indicated. 903: UACC903, 9036: UACC903(+6), 903UV: UACC903 treated with UV, 9036UV: UACC903(+6) treated with UV

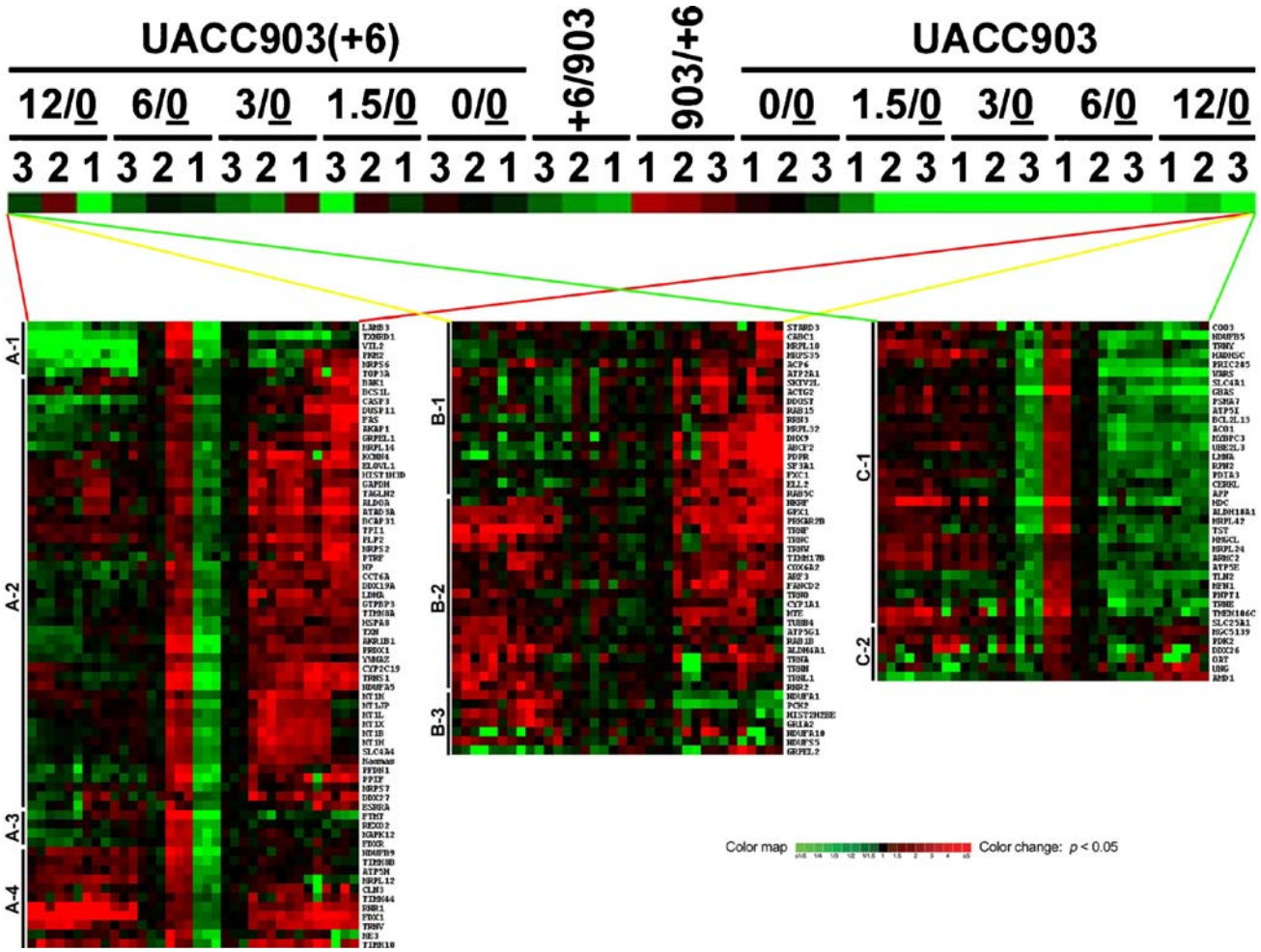

Fig. 2 Heat map of gene expression. UACC903(+6) and UACC903 cells were treated with or without the UV irradiation. The "0" indicates that the cells were harvested with the mock treatment, that is, without UV irradiation. Other cells were harvested at 1.5-, 3-, 6- and 12-h time points after the UV treatment. The samples were arranged on the top as such to reveal a symmetrical comparison between UACC903(+6) and UACC903 and a timing course for each cell line after the UV treatment. The expression ratios between UACC903(+6) and UACC903 (+6/903 and 903/+6) were calculated and placed in the middle for the symmetric clustering analysis. The '0/0' is calculated by dividing an individual value with the mean value at the 0 time point, which provides the control reference (black) for up- (red) and down- (green) regulation or no-change in expression (black) of a gene. The UV-induced expression changes were calculated by comparisons of a gene expression level at each time point with the mean value at the 0 time point, that is, 1.5/0, 3/0, 6/0 and 12/0. The triplicate experiments (indicated as 1, 2, 3) were performed for each time point. The clusters without UV treatment are indicated by (**a**) 68 genes with expression levels significantly ($P < 0.05$) higher in UACC903(+6) cell line than in UACC903, (**b**) 47 genes without significant ($P > 0.05$) changes between these two cell line, and (**c**) 39 genes with expression levels significantly ($P < 0.05$) lower in UACC903(+6) than in UACC903. The sub-clusters (A-1 through A-4, B-1 through B-3, C-1 and C-2) indicate the UV-induced changes in expression. The gene symbols are indicated and please see website http://www.gwumc.edu/biochem/faculty/su.html for gene IDs and names

to and lower than those in UACC903, respectively. At 1.5-, 3-, 6- and 12-h after UV treatment, genes in all 9 sub-clusters displayed significant ($P < 0.05$) up- or down-regulation at more than one time point, in either one cell line or both. These sub-clusters revealed downregulated (A-1) and upregulated (A-4 and B-2) genes in both cell lines, upregulated genes in UACC903(+6) (B-3 and C-1) and UACC903 (A-2 and B-1), and a mixture of both up- and down-regulated genes (A-3 and C-2), in response to the UV treatment (Fig. 2).

qRT-PCR validation of gene expression

To validate the microarray results, we conducted qRT-PCR analysis on 11 genes including proapoptotic genes (BAK1, FAS and CASP3), antiapoptotic genes (BCL2L1 and MCL1), DNA damage repair genes (FANCD2 and UNG), others (AMD1, DHX16 and PPP2CA) and the control GAPDH, in UACC903 and UACC903(+6) cell lines before (0-h) and at 3- and 12-h after the UV treatment. The results indicated that out of 30 datapoints tested (10 genes

at 3 time-points, $n = 30$), 28 (93.3%) were in agreement with the microarray results, including 21 (70%) with agreement in both change (down, no change, or up) and significance ($P <$ or > 0.05) and 7 (23.3%) with agreement in change but not in significance (Fig. 3). The expression of 2 genes (6.7%) was inconsistent and included BAK1 at the 0-h time point and MCL1 at the 3-h time point (Fig. 3). These results demonstrated overall agreement between the microarray data and the qRT-PCR results. Thus, all 154 genes were subjected to further analysis.

Expression patterns of genes involved in proapoptosis (16 genes), antiapoptosis (3 genes), DNA damage repair (5 genes) and G2 checkpoint (1 gene) before and after UV treatment

To find genes controlling key phenotypic differences (i.e., apoptosis and G2/M phase transition [Fig. 1]) between UACC903(+6) and UACC903 cells, our ontology analysis of the 154 differentially expressed genes revealed 16 proapoptotic genes, 3 antiapoptotic genes, 1 G2 checkpoint gene, and 5 DNA damage repair genes (Fig. 4a). Without UV treatment, 10 proapoptotic genes (FDX1, BCAP31, BNIP1, VDAC1, FDXR, BAK1 [encoded by 6p21.3], TNFSF10, FAS, CASP6 and CASP3) were all upregulated in UACC903(+6) and downregulated in UACC903, while the expression of 5 proapoptotic genes (BAD, BID, BBC3, CYCS and APAF1) displayed no significant change. In response to the UV treatment, significantly ($P < 0.05$) upregulated FDX1, BAD and BID, downregulated FDXR, BAK1, TNFSF10, FAS, CASP6, CASP3 and APAF1, and insignificantly changed BCAP31, BNIP1, VDAC1, BBC3 and CYCS were identified in UACC903(+6) cells. In comparison, identification in UACC903 cells of significantly upregulated 12 genes (FDX1, BCAP31, BNIP1, VDAC1, FDXR, BAK1, TNFSF10, FAS, CASP6, CASP3, BBC3 and CYCS), downregulated APAF1, and did not change BAD and BID (Fig. 4a) were noted. Without UV treatment, 3 antiapoptotic genes (CLN3, MCL1 and BCL2L1) were upregulated in UACC903(+6) and downregulated in UACC903. The UV treatment induced downregulation of MCL1 and BCL2L1 in UACC903(+6) and upregulation of all 3 genes in UACC903. CLN3 expression in UACC903(+6) did not respond to UV irradiation (Fig. 4a).

Five genes with DNA damage repair function, including FANCD2, APEX1, APEX2, UNG and TP53, displayed no significant changes in expression between UACC903(+6) and UACC903 without UV treatment. In contrast, FANCD2, APEX1 and APEX2 were all upregulated in UACC903 in response to UV treatment (Fig. 4a). FANCD2 is also required to maintain the DNA damage-induced G2 checkpoint. UNG expression was downregulated in UACC903(+6) cells at the 3-h time point but

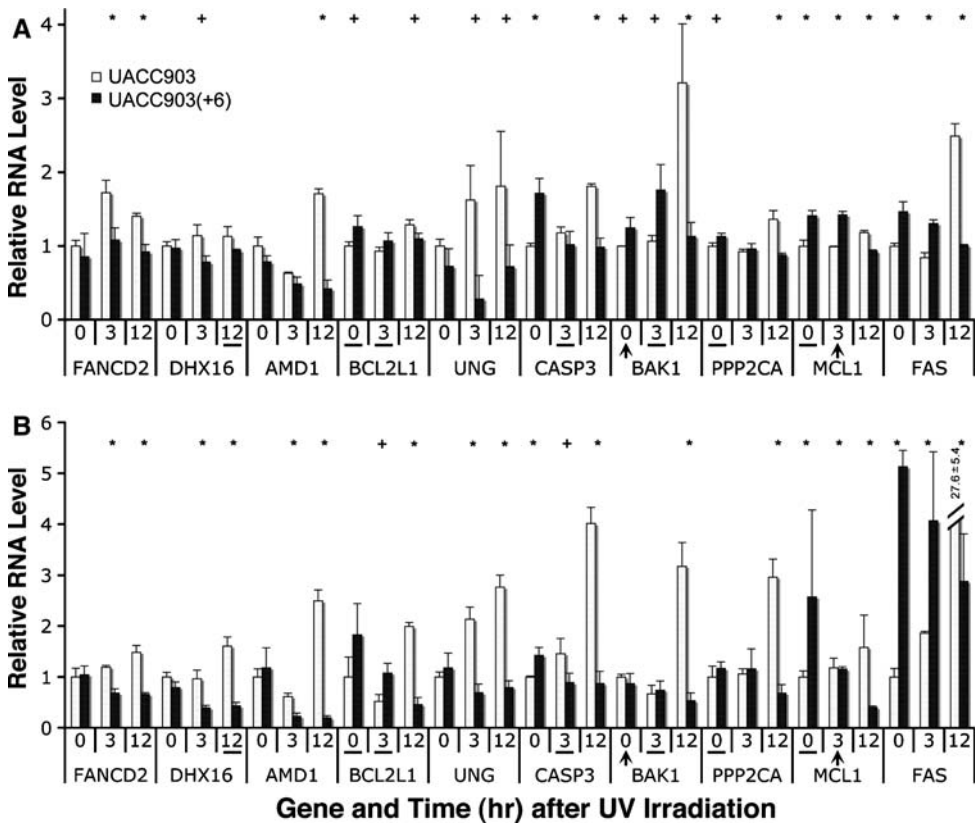

Fig. 3 Consistent RNA levels measured by microarray and qRT-PCR. (**a**) Relative RNA ratios of 10 genes, each at 3 time points, between UACC903 and UACC903(+6) cell lines measured by microarrays. (**b**) Relative RNA levels of the same 10 genes, each at the same 3 time points, measured by qRT-PCR. The '+' sign indicates $P < 0.05$, and the '*' indicates $P < 0.01$ for a pair within measurement. Out of these 30 gene-and-time-point comparisons, 28 (93.3%) are consistent between these two types of measurements, including 21 (70%) with agreement in both change (down, no, or up) and *P*-value, and 7 (23.3%) consistent with the changes but not with *P*-value (underlined). Two (6.7%) was inconsistent and included BAK1 at 0-h time point and MCL1 at 3-h time point (arrowhead)

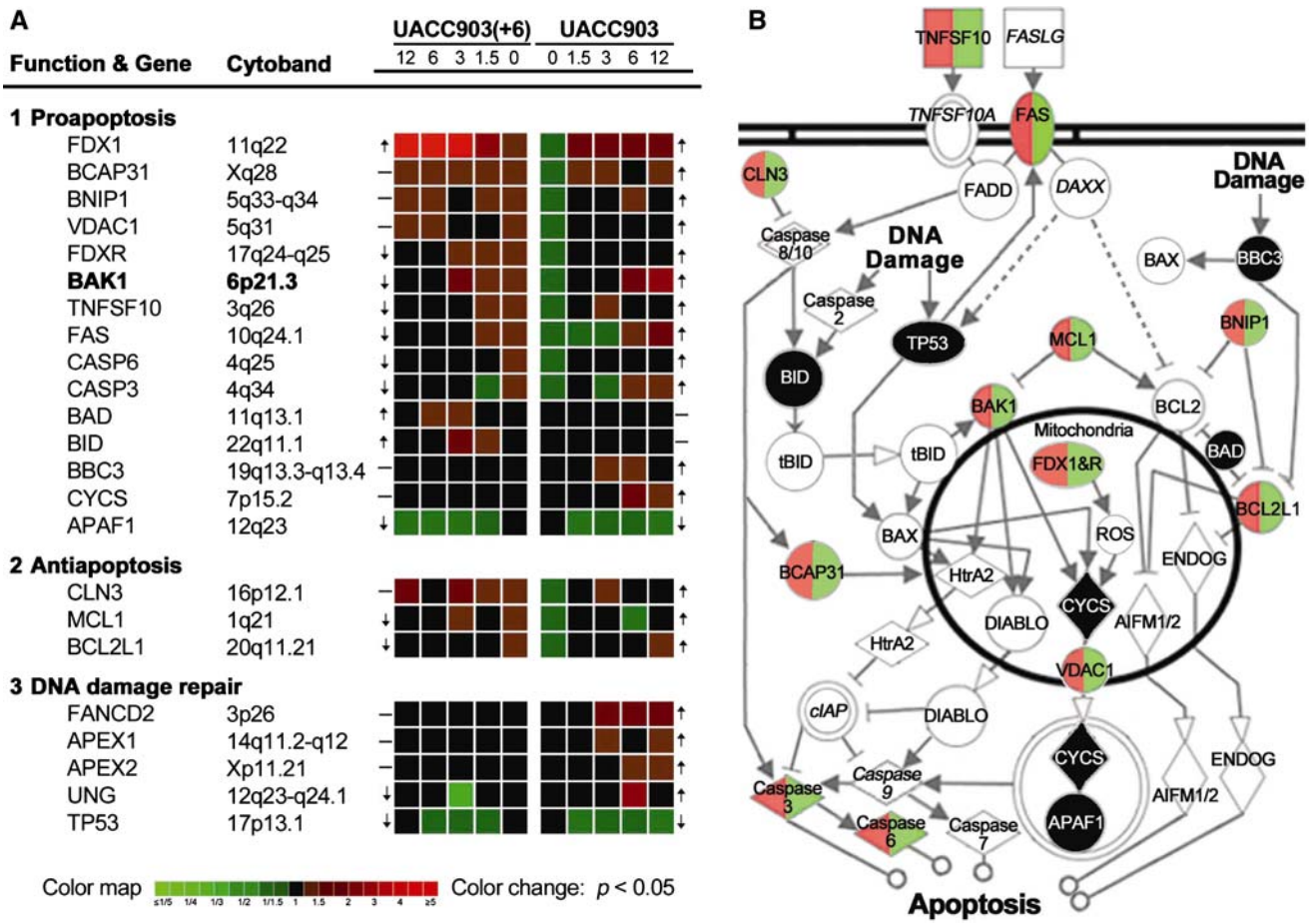

Fig. 4 Heat map and survival-apoptosis pathways. (**a**) Heat map of 15 proapoptotic, 3 antiapoptotic, and 5 DNA-damage-repair genes in UACC903(+6) and UACC903 cell lines before (0) and at 1.5-, 3-, 6-, and 12-h after the UV treatment. The color map illustrates a color change corresponding to a ratio change. Each ratio was calculated by dividing an expression level of a given gene at the time point to the mathematic mean value of the gene expression levels in both UACC903(+6) and UACC903 cells without UV treatment. The arrowheads and hyphens indicate overall expression changes of a gene in response to the UV treatment. (**b**) The survival-apoptosis pathways with differentially expressed genes between UACC903(+6) and UACC903 cell lines without UV treatment. Red, green and black correspond to those at the 0-h time point in UACC903(+6) and UACC903 cell line listed in the panel (A). The left and right half in each gene plate represents relative expression levels between UACC903(+6) and UACC903, respectively. Solid line with solid arrowhead: direct activation of expression or activity; dashed line: indirect; open arrowhead: translocation; line with a short line at one end: inhibition; line with circle: leading to; square: cytokine; double circles or rhombus: group or complex; rhombus: enzymes; circle: named protein; membrane: cell membrane

upregulated in UACC903 cells at the 6-h time point. Although TP53 is known to be involved in both apoptosis and DNA damage repair, its expression was downregulated in both cell lines in response to UV treatment (Fig. 4a).

Survival-apoptosis signaling pathways with differentially expressed genes ($n = 19$) in UACC903(+6) and UACC903 cells before and after UV treatment

We mapped the aforementioned 16 proapoptosis genes and 3 antiapoptosis genes to known molecular signaling pathways that regulate survival and apoptosis of cells. The results revealed mitochondria-centered signaling pathways with a total of 35 gene products (Fig. 4b). Without UV irradiation, the expression of 10 proapoptotic genes (TNFSF10, FAS, BNIP1, BAK1 [encoded by 6p21.3], BCAP31, FDX1, FDXR, VDAC1, CASP6 and CASP3) and 3 antiapoptotic genes (BCL2L1, CLN3 and MCL1) were significantly ($P < 0.05$) higher in the UACC903(+6) cell line (red) than in UACC903 (green). Six genes (BBC3, BID, TP53, BAD, CYCS and APAF1) had no significant change in expression (black). Expression changes of 11 genes (FADD, CASP8, CASP10, CASP2, BAX, HtrA2, DIABLO, AIFM1, AIFM2, ENDOG, CASP7) were not detected. The expression status of the remaining 5 genes (FASLG, TNFSF10A, DAXX, IAP and CASP9) was unknown (italic) due to the absence from the microarray.

The known interactions of these genes are indicated in the pathways. The differential gene expression pattern in these survival-apoptosis signaling pathways appears to predict the UACC903(+6) cell line's sensitivity, compared to the UACC903's resistance to apoptosis (Fig. 4b).

Validation of expression changes of proapoptotic (BAK1 and FAS) and antiapoptotic (BCL2L1 and MCL1) proteins

To correlate mRNA levels to protein expression, Western blot analysis of proapoptotic proteins (BAK1 and FAS), antiapoptotic proteins (BCL2L1 and MCL1), and control (GAPDH) was performed for these two cell lines before and after UV treatment. The relative protein levels from two independent Western blots were scanned and normalized to GAPDH. The results indicated that without UV treatment the protein levels of BAK1, BCL2L1 and FAS were at least threefold higher and the MCL1 protein was 1.6-fold greater in UACC903(+6) cells than in UACC903 (Fig. 5). After the UV treatment these proteins maintained high expression levels in UACC903(+6), with some decrease of BAK1, BCL2L1 and FAS proteins at 6- and 12-h time points. In comparison, all 4 proteins in UACC903 remained the same or were modestly reduced at 1.5-, 3- and 6-h time points, while increasing slightly at the 12-h time point (Fig. 5).

Functional validation of the differential survival-apoptosis signaling pathways

To validate the survival-apoptosis signaling pathways, we performed MTS cell proliferation assays comparing viability after parallel treatment of UACC903(+6) and UACC903 cells with FASLG. The results indicated that cell survival was a function of dose and time following FASLG

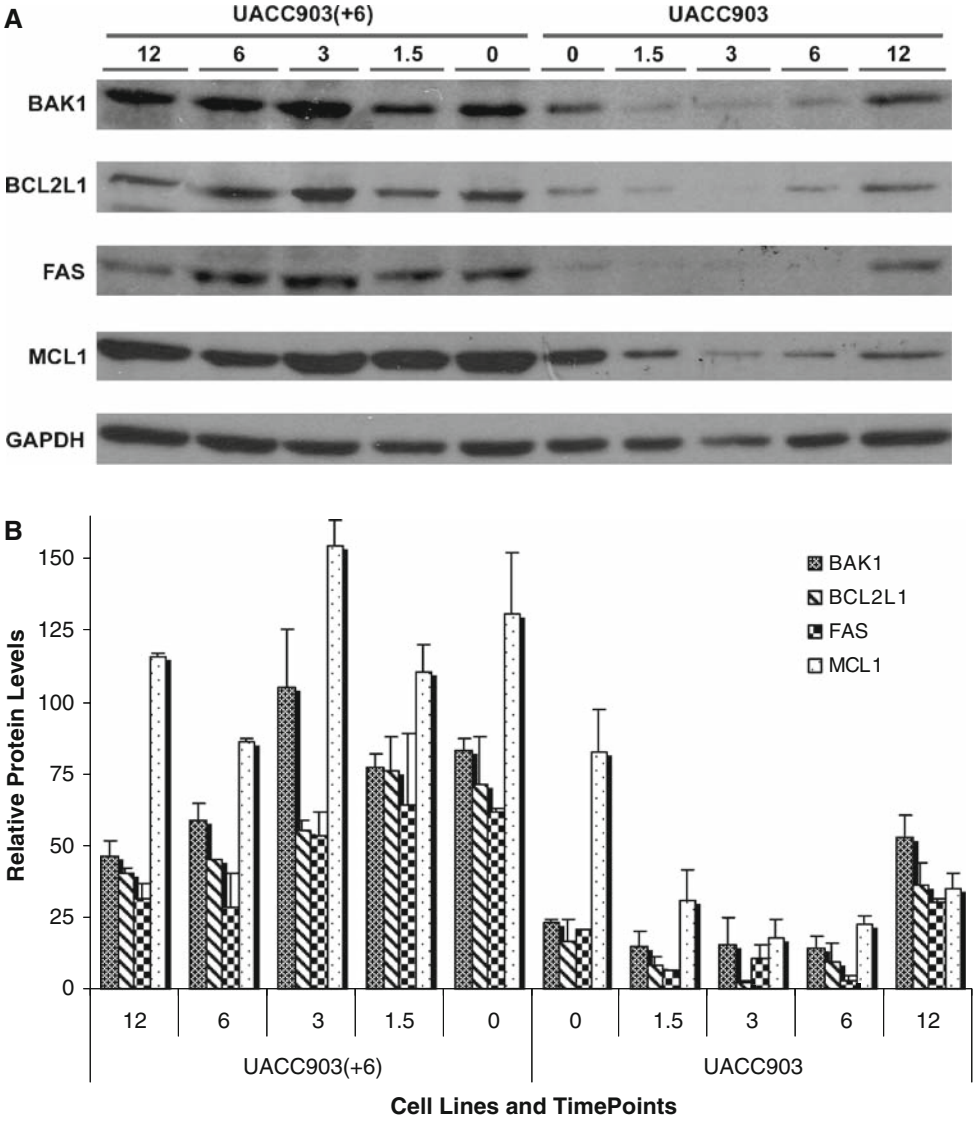

Fig. 5 Western blots and quantification. (**a**) Western blot of cell lysate from UACC903(+6) and UACC903 cell lines before (0) and at 1.5-, 3-, 6-, and 12-h after the UV treatment, using the antibodies against BAK1, BCL2L1, FAS, MCL1 and GAPDH proteins. GAPDH was used as a control for loading error. (**b**) Bar graph for the quantitative comparison among protein expression levels. The signal intensities of a protein band and its surrounding background were scanned from images derived from two independent Western experiments for each protein and quantified by using Scanalytics IPLAB 3.6 (Rockville, MD). The resultant background-subtracted values of protein expression were normalized to those of GAPDH and then plotted as the relative protein levels for each protein at each time point in each cell line with or without UV treatment

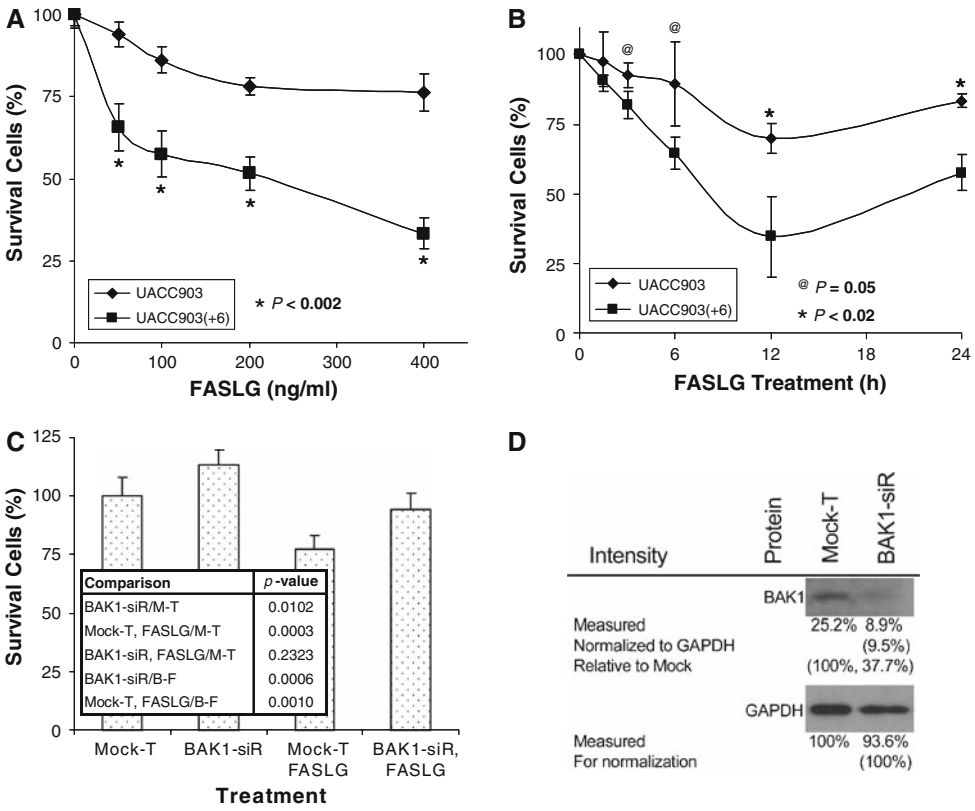

Fig. 6 Survival analysis of UACC903(+6) and UACC903 cell lines. (**a**) Survival curves of UACC903(+6) and UACC903 cells in response to FAS ligand (FASLG) at the doses of 50, 100, 200, and 400 ng/ml. (**b**) time–response curves of the cells to the treatment with 100 ng/ml of FASLG. (**c**) Effects of the siRNA knockdown of BAK1 protein on survival of UACC903(+6) cells following BAK1 siRNA transfection. (**d**) Western blot analysis of BAK1 protein levels in UACC903(+6) cells following BAK1 siRNA transfection. Mock-T (M-T): mock transfection with no-specific siRNA; siR:siRNA; B-F: BAK1-siR—FASLG

treatment, and that the survival of UACC903(+6) cells was significantly less than that of UACC903 (Fig. 6a and b). Specifically, at the dose of 50, 100, 200, or 400 ng/ml FASLG, UACC903(+6) cells had 66 ± 7.1%, 57 ± 7.0%, 52 ± 5.0% and 33 ± 4.7% survival, but UACC903 had 94 ± 3.8%, 86 ± 3.9%, 78 ± 2.7% and 76 ± 5.5% survival, respectively. The difference at each corresponding dose was highly significant ($P < 0.002$). At 1.5-, 3-, 6-, 12- and 24-h after treatment with 100 ng/ml FASLG, the UACC903(+6) cell survival was reduced to 91 ± 1.9%, 82 ± 4.9%, 64 ± 5.8%, 35 ± 14.4%, and 58 ± 6.5%, respectively; while the corresponding UACC903 cell survival was 98 ± 10.6%, 93 ± 4.4%, 90 ± 15.2%, 70 ± 5.4% and 83 ± 2.4%. The survival difference between these two cell lines was insignificant ($P = 0.332$) at the 1.5-h time point, significant at 3- and 6-h time points ($P = 0.050$), and highly significant at 12-h ($P = 0.016$) and 24-h ($P = 0.003$) time points (Fig. 6a and b).

To further validate the survival-apoptosis signaling pathway, we determined the effects of siRNA knockdown of the proapoptotic protein BAK1 on survival of UACC903(+6) cells in the presence or absence of FASLG. The results indicate that transfection with BAK1 siRNA (BAK1-siR) significantly ($P = 0.0102$) increased cell survival by 114 ± 6.4% greater than mock transfection (100 ± 8.3%). Western blot analysis indicated that BAK1 protein was knocked down to 37.7% of mock transfection. Moreover, in the absence of BAK1 siRNA, FASLG-induced cell death was 77 ± 6.0% ($P = 0.0003$); whereas in the presence, the FASLG-induced cell death was 94 ± 7.0% which is insignificantly different from mock transfection ($P = 0.2323$), but highly significantly different from the treatment with either BAK1 siRNA (114 ± 6.4%, $P = 0.0006$) or FASLG (77 ± 6.0%, $P = 0.0010$) alone (Fig. 6c and d).

Discussion

This study identified survival-apoptosis molecular signaling pathways with differentially expressed genes underlying resistance and sensitivity to apoptosis of human malignant melanoma cell line UACC903 and the chromosome 6-mediated suppressed cell line UACC903(+6). UACC903 cells displayed resistance to apoptosis and G2/M arrest at significantly higher levels than UACC903(+6) regardless of UV treatment. In contrast, UACC903(+6) cells had a low level of constitutive apoptosis, which increased by >5-fold in response to UV irradiation (Fig. 1). By applying human mitochondria-focused cDNA microarrays, we identified the difference in the survival-apoptosis signaling pathways between these two cell lines (Fig. 4). The expression changes of a number of representative genes were validated by qRT-PCR and Western

blots. The FASLG-induced dose- and time-responsive cell deaths were exploited to functionally validate the differential survival-apoptosis signaling pathways. Moreover, siRNA knockdown of the upregulated proapoptotic protein BAK1, encoded at chromosome 6p21.3, in UACC903(+6) cells not only enhanced cell survival, but also attenuated FASLG-induced cell death further validating this pathway. Thus, the identified differential survival-apoptosis signaling pathways provide a molecular mechanism underlying resistance and sensitivity to apoptosis of these two melanoma cell lines (UACC903 and UACC903[+6]).

The survival-apoptosis molecular signaling pathway contains gene products involved in multiple proapoptotic and antiapoptotic signaling pathways, including extrinsic and intrinsic, caspase-dependent and -independent, mitochondria-centered, and other organelle-related paths. Homeostasis between proapoptosis and antiapoptosis may be a key factor regulating life and death of cells [26–28]. For example, in the extrinsic, caspase-dependent apoptosis pathway, the proapoptotic proteins TNFSF10 and FAS are known to induce apoptosis as immune response, through activation of CASP8 and CASP10, which in turn activate CASP3 and CASP6, leading to apoptosis. The UACC903 cell line's significantly lower expression of 10 proapoptotic genes (in contrast to only 3 antiapoptotic genes) than the UACC903(+6) cell line may explain why the former had fewer constitutive and UV- or FASLG-induced cell deaths than the latter. Apparently, multiple proteins in the survival-apoptosis signaling pathways participate in the resistance of UACC903 and the sensitivity of UACC903(+6) to apoptosis. The approach employed and pathways identified by this study may facilitate therapeutic research aimed at discovery of drugs and drug targets.

The FAS and FASLG system comprises a major pathway for the induction of apoptosis in cells and tissues that play central roles in the physiological regulation of tissue remodeling, the pathogenesis of various malignancies, and diseases of the immune response. FAS, also known as TNFRSF6/APT1/CD95, is a cell surface receptor and a member of the tumor necrosis factor (TNF)-receptor superfamily. Its ligand FASLG, also known as TNFSF6/APT1LG1/CD95L, can trigger apoptosis by cross-linking with FAS [29, 30]. Since FAS-FASLG signaling is necessary and sufficient to control keratinocyte apoptosis of the epidermis exposed to UV-light, it thus plays a crucial role in regulation of UV-induced DNA damage-triggered apoptosis [31].

Our study reveals that the FAS-FASLG signaling pathway, which interacts with the DNA damage-triggered apoptosis pathway, consists of multiple genes with altered expression between human malignant melanoma cell line UACC903 and the suppressed cell line UACC903(+6). Significantly more UACC903 cells arrest in the G2/M phase, constitutive and UV-induced, than UACC903(+6) cells. The UV treatment causes damage to DNA; and cells with excessive DNA damage undergo apoptosis, preventing abnormal growth [32, 33]. The G2/M-arrest, particularly the arrested UACC903 cells induced by the UV irradiation, may undergo DNA damage repair. This hypothesis is supported by the fact that genes involved in the cell cycle G2 checkpoint (FANCD2) [34] and DNA damage repair (FANCD2, APEX1, APEX2 and UNG) were all upregulated in the UV-treated UACC903 cells. In contrast, none of these genes responded to UV treatment in UACC903(+6) cells (Fig. 4a). It is known that FANCD2 protein involves in the homology-directed DNA repair [35, 36], APEX1 and APEX2 repair apurinic/apyrimidinic sites [37, 38], and UNG initiates the base-excision repair (BER) [39]. These genes provide molecular clues for further study of G2/M arrest and DNA damage repair that may play a key role in development of human malignant melanomas.

In the present study, we found striking UV-induced changes in expression patterns between the UACC903(+6) and UACC903 cell lines. The unsupervised clustering analysis of 154 genes revealed 3 clusters and 9 sub-clusters of genes. The fact that at least 4 sub-clusters (A-2, B-1, B-3 and C-1) consisting of 104 genes displayed significantly different expression patterns between these two cell lines in response to the UV treatment (Fig. 2) strongly suggests the different regulatory mechanisms controlling expression of these genes. Differences in expression of so many genes suggest the presence of different control mechanisms underlying expression of these genes, either directly or through cascade effect. Probably, all of these differentially expressed genes contribute to the phenotypic differences between the malignant melanoma cell line UACC903 and the chromosome 6-mediated suppressed cell line UACC903(+6).

Changes in protein expression lag behind RNA changes. The comparisons between RNA expression and protein expression of four genes including BAK1, BCL2L1, FAS and MCL1 indicate that the RNA changes occurred earlier than the protein in response to UV treatment (Figs. 4a and 5). In addition, the changes in expression patterns of BAK1, BCL2L1, FAS and MCL1 RNA and protein were very similar. These results suggest that these 4 genes may be regulated at both transcriptional and translational levels in response to UV treatment.

To date, a number of genes encoded by human chromosome 6 have been shown to be involved in chromosome 6-mediated suppression of CMM phenotypes. Church et al. identified the mitochondrial antioxidant enzyme manganese superoxide dismutase 2 (SOD2) (6q25.3) as a tumor suppressor gene that inhibits colony formation in soft agar and tumors in nude mice [40]. Our previous study revealed

up- and down-regulation of gap junction protein alpha 1 (GJA1) (6q21-q23.2), also known as connexin 43 (Cx43), in UACC903(+6) and UACC903, respectively, and demonstrated the suppression of colony formation of UACC903 cells in soft agar by transfection and overexpression of GJA1 [17]. Other investigators reported that GJA1 inhibits proliferation of glioblastoma cell lines [41], lung carcinoma cell line PG [42], prostate cancer cell line LNCap [43] and breast cancer cell line MDA-MB-231 [44] in vitro and in nude mice. Goldberg et al discovered the transcriptional coactivator CRSP3/MED23 (6q22.33-q24.1) as a metastasis suppressor by upregulation of a metastasis suppressor gene KISS1 [45]. In the current study we demonstrated that upregulation of BAK1 (6p21.3) RNA and protein was associated with the UACC903(+6) cell line's sensitivity to apoptosis, and that siRNA downregulation of BAK1 protein led to an increase in the cell survival. Taken together, all these studies demonstrated that chromosome 6-mediated tumor suppression involves an abnormal expression of genes to regulate survival (i.e., SOD2), apoptosis (i.e., BAK1), proliferation (i.e., GJA1), and transcription (i.e., CRSP3). These complex molecular changes may be different in different genetic backgrounds or cancer cells. Accordingly, this type of heterogeneity requires the genomic and proteomic studies of an individual clone of cancer cells derived from different (or even the same) patients for complete mapping and understanding of the molecular basis underlying the cell behavior, and for the development of diagnostic and/or therapeutic methods.

Acknowledgments The authors thank Dan Sackett for his critical review of the manuscript. This work was supported by NIH-NIDDK-06-925, the Catherine B McCormick Genomics Center, and a gift from the St. Laurent Institute. P.H. was supported by Division of Hematology, Center for Biological Evaluation and Research, Food and Drug Administration. O.M.R. was supported by Program in Reproductive and Adult Endocrinology, Laboratory of Clinical Genomics, Eunice Kennedy Shriver National Institute of Child Health and Human Development, National Institutes of Health. Authors state that there are no any competing financial, professional, or personal conflicts of interest related to this publication.

References

1. American Cancer Society (2007) Cancer facts and figures 2007. American Cancer Society, Atlanta, pp 1–54
2. Gray-Schopfer V, Wellbrock C, Marais R (2007) Melanoma biology and new targeted therapy. Nature 445:851–857. doi:10.1038/nature05661
3. Meier F, Satyamoorthy K, Nesbit M et al (1998) Molecular events in melanoma development and progression. Front Biosci 3:D1005–D1010
4. Kim R, Emi M, Tanabe K (2006) The role of apoptosis in cancer cell survival and therapeutic outcome. Cancer Biol Ther 5:1429–1442
5. Su YA, Trent JM (1995) Genetics of cutaneous malignant melanoma. Cancer Control 2:392–397
6. Thompson FH, Emerson J, Olson S et al (1995) Cytogenetics of 158 patients with regional or disseminated melanoma. Subset analysis of near-diploid and simple karyotypes. Cancer Genet Cytogenet 83:93–104. doi:10.1016/0165-4608(95)00057-V
7. Sargent LM, Nelson MA, Lowry DT et al (2001) Detection of three novel translocations and specific common chromosomal break sites in malignant melanoma by spectral karyotyping. Genes Chromosomes Cancer 32:18–25. doi:10.1002/gcc.1162
8. Pathak S, Drwinga HL, Hsu TC (1983) Involvement of chromosome 6 in rearrangements in human malignant melanoma cell lines. Cytogenet Cell Genet 36:573–579
9. Trent JM, Thompson FH, Meyskens FL Jr (1989) Identification of a recurring translocation site involving chromosome 6 in human malignant melanoma. Cancer Res 49:420–423
10. Millikin D, Meese E, Vogelstein B et al (1991) Loss of heterozygosity for loci on the long arm of chromosome 6 in human malignant melanoma. Cancer Res 51:5449–5453
11. Walker GJ, Palmer JM, Walters MK et al (1994) Simple tandem repeat allelic deletions confirm the preferential loss of distal chromosome 6q in melanoma. Int J Cancer 58:203–206. doi:10.1002/ijc.2910580210
12. Trent JM, Stanbridge EJ, McBride HL et al (1990) Tumorigenicity in human melanoma cell lines controlled by introduction of human chromosome 6. Science 247:568–571. doi:10.1126/science.2300817
13. Welch DR, Chen P, Miele ME et al (1994) Microcell-mediated transfer of chromosome 6 into metastatic human C8161 melanoma cells suppresses metastasis but does not inhibit tumorigenicity. Oncogene 9:255–262
14. Miele ME, Robertson G, Lee JH et al (1996) Metastasis suppressed, but tumorigenicity and local invasiveness unaffected, in the human melanoma cell line MelJuSo after introduction of human chromosomes 1 or 6. Mol Carcinog 15:284–299. doi : 10.1002/(SICI)1098-2744(199604)15:4<284::AID-MC6>3.0.CO;2-G
15. Zhang Q, Chen Y, Wang BD et al (2007) Differences in apoptosis and cell cycle distribution between human melanoma cell lines UACC903 and UACC903(+6), before and after UV irradiation. Int J Biol Sci 3:342–348
16. Su YA, Ray ME, Lin T et al (1996) Reversion of monochromosome-mediated suppression of tumorigenicity in malignant melanoma by retroviral transduction. Cancer Res 56:3186–3191
17. Su YA, Bittner ML, Chen Y et al (2000) Identification of tumor-suppressor genes using human melanoma cell lines UACC903, UACC903(+6), and SRS3 by comparison of expression profiles. Mol Carcinog 28:119–127. doi :10.1002/1098-2744(200006)28:2<119::AID-MC8>3.0.CO;2-N
18. Bai X, Wu J, Zhang Q et al (2007) Third-generation human mitochondria-focused cDNA microarray and its bioinformatic tools for analysis of gene expression. Biotechniques 42:365–375
19. Darzynkiewicz Z, Li X, Gong J (1994) Assays of cell viability: discrimination of cells dying by apoptosis. Methods Cell Biol 41:15–38
20. Vermes I, Haanen C, Steffens-Nakken H et al (1995) A novel assay for apoptosis. Flow cytometric detection of phosphatidylserine expression on early apoptotic cells using fluorescein labelled Annexin V. J Immunol Methods 184:39–51. doi:10.1016/0022-1759(95)00072-I

21. Gavrieli Y, Sherman Y, Ben-Sasson SA (1992) Identification of programmed cell death in situ via specific labeling of nuclear DNA fragmentation. J Cell Biol 119:493–501. doi:10.1083/jcb.119.3.493
22. Ben-Sasson SA, Sherman Y, Gavrieli Y (1995) Identification of dying cells—in situ staining. Methods Cell Biol 46:29–39. doi:10.1016/S0091-679X(08)61922-6
23. Manoli I, Le H, Alesci S et al (2005) Monoamine oxidase-A is a major target gene for glucocorticoids in human skeletal muscle cells. FASEB J 19:1359–1361
24. Eisen MB, Spellman PT, Brown PO et al (1998) Cluster analysis and display of genome-wide expression patterns. Proc Natl Acad Sci USA 95:14863–14868. doi:10.1073/pnas.95.25.14863
25. Holland PM, Abramson RD, Watson R et al (1991) Detection of specific polymerase chain reaction product by utilizing the 5′-3′ exonuclease activity of Thermus aquaticus DNA polymerase. Proc Natl Acad Sci USA 88:7276–7280. doi:10.1073/pnas.88.16.7276
26. Belizario JE, Alves J, Occhiucci JM et al (2007) A mechanistic view of mitochondrial death decision pores. Braz J Med Biol Res 40:1011–1024. doi:10.1590/S0100-879X2006005000109
27. Eberle J, Fecker LF, Hossini AM et al (2008) Apoptosis pathways and oncolytic adenoviral vectors: promising targets and tools to overcome therapy resistance of malignant melanoma. Exp Dermatol 17:1–11. doi:10.1159/000109583
28. Kulms D, Schwarz T (2002) Mechanisms of UV-induced signal transduction. J Dermatol 29:189–196. doi:10.1159/000065313
29. Sharma K, Wang RX, Zhang LY et al (2000) Death the Fas way: regulation and pathophysiology of CD95 and its ligand. Pharmacol Ther 88:333–347. doi:10.1016/S0163-7258(00)00096-6
30. Kavurma MM, Khachigian LM (2003) Signaling and transcriptional control of Fas ligand gene expression. Cell Death Differ 10:36–44. doi:10.1038/sj.cdd.4401179
31. Guzman E, Langowski JL, Owen-Schaub L (2003) Mad dogs, Englishmen and apoptosis: the role of cell death in UV-induced skin cancer. Apoptosis 8:315–325. doi:10.1023/A:1024112231953
32. Wei Q, Lee JE, Gershenwald JE et al (2003) Repair of UV light-induced DNA damage and risk of cutaneous malignant melanoma. J Natl Cancer Inst 95:308–315
33. Banerjee G, Gupta N, Kapoor A et al (2005) UV induced bystander signaling leading to apoptosis. Cancer Lett 223:275–284. doi:10.1016/j.canlet.2004.09.035
34. Freie BW, Ciccone SL, Li X et al (2004) A role for the Fanconi anemia C protein in maintaining the DNA damage-induced G2 checkpoint. J Biol Chem 279:50986–50993. doi:10.1074/jbc.M407160200
35. Garcia-Higuera I, Taniguchi T, Ganesan S et al (2001) Interaction of the Fanconi anemia proteins and BRCA1 in a common pathway. Mol Cell 7:249–262. doi:10.1016/S1097-2765(01)00173-3
36. Hussain S, Wilson JB, Medhurst AL et al (2004) Direct interaction of FANCD2 with BRCA2 in DNA damage response pathways. Hum Mol Genet 13:1241–1248. doi:10.1093/hmg/ddh135
37. Chou KM, Cheng YC (2002) An exonucleolytic activity of human apurinic/apyrimidinic endonuclease on 3′ mispaired DNA. Nature 415:655–659. doi:10.1038/415655a
38. Burkovics P, Szukacsov V, Unk I et al (2006) Human Ape2 protein has a 3′-5′ exonuclease activity that acts preferentially on mismatched base pairs. Nucleic Acids Res 34:2508–2515. doi:10.1093/nar/gkl259
39. Kavli B, Sundheim O, Akbari M et al (2002) hUNG2 is the major repair enzyme for removal of uracil from U:A matches, U:G mismatches, and U in single-stranded DNA, with hSMUG1 as a broad specificity backup. J Biol Chem 277:39926–39936. doi:10.1074/jbc.M207107200
40. Church SL, Grant JW, Ridnour LA et al (1993) Increased manganese superoxide dismutase expression suppresses the malignant phenotype of human melanoma cells. Proc Natl Acad Sci USA 90:3113–3117. doi:10.1073/pnas.90.7.3113
41. Huang RP, Fan Y, Hossain MZ et al (1998) Reversion of the neoplastic phenotype of human glioblastoma cells by connexin 43 (cx43). Cancer Res 58:5089–5096
42. Zhang ZQ, Zhang W, Wang NQ et al (1998) Suppression of tumorigenicity of human lung carcinoma cells after transfection with connexin43. Carcinogenesis 19:1889–1894. doi:10.1093/carcin/19.11.1889
43. Mehta PP, Perez-Stable C, Nadji M et al (1999) Suppression of human prostate cancer cell growth by forced expression of connexin genes. Dev Genet 24:91–110. doi :10.1002/(SICI)1520-6408(1999)24:1/2<91::AID-DVG10>3.0.CO;2-#
44. Qin H, Shao Q, Curtis H et al (2002) Retroviral delivery of connexin genes to human breast tumor cells inhibits in vivo tumor growth by a mechanism that is independent of significant gap junctional intercellular communication. J Biol Chem 277:29132–29138. doi:10.1074/jbc.M200797200
45. Goldberg SF, Miele ME, Hatta N et al (2003) Melanoma metastasis suppression by chromosome 6: evidence for a pathway regulated by CRSP3 and TXNIP. Cancer Res 63:432–440